

GINGA OBSERVATIONS OF QUASI-PERIODIC OSCILLATIONS IN TYPE II BURSTS FROM THE RAPID BURSTER

T. DOTANI, K. MITSUDA, H. INOUE, AND Y. TANAKA
 Institute of Space and Astronautical Science, Kanagawa, Japan

N. KAWAI
 Cosmic Radiation Laboratory, RIKEN Institute of Physical and Chemical Research, Saitama, Japan

Y. TAWARA
 Department of Astrophysics, Faculty of Science, Nagoya University, Japan

K. MAKISHIMA
 Department of Physics, University of Tokyo, Japan

J. VAN PARADIJS, W. PENNINX, AND M. VAN DER KLIS
 Astronomical Institute "Anton Pannekoek," University of Amsterdam, the Netherlands and Center for High Energy Astrophysics, Amsterdam

AND

J. TAN AND W. H. G. LEWIN
 Center for Space Research and Department of Physics, Massachusetts Institute of Technology
 Received 1989 May 17; accepted 1989 August 9

ABSTRACT

During *Ginga* observations of the "Rapid Burster" in 1988 August, we detected strong quasi-periodic oscillations (QPOs) in its X-ray intensity. The QPOs had centroid frequencies of ~ 5 , and ~ 2 Hz during type II X-ray bursts which lasted for ~ 10 and 30 s, respectively. No QPOs were found in the persistent X-ray emission between the bursts. The presence of the QPOs is correlated with the time scale-invariant burst profile: they are very strong during the initial peak in the burst, absent in the second peak, and strong again at the onset of the third peak (average rms variations of $17.6 \pm 1.6\%$, $< 2\%$, and $12.5 \pm 1.8\%$, respectively). The amplitude of the 5 Hz QPO is very large, and individual oscillations are easily seen in the X-ray intensity curve. From the times of maximum intensity of the oscillations that are seen during the initial peaks of ~ 60 type II bursts, we find that during the large majority of the bursts the oscillations can be described as periodic modulations without phase jumps, whose frequencies change gradually by up to $\sim 25\%$ during a burst. In most cases, the frequency decreases; however, frequency increase and both decrease and increase of frequency have also been observed. These frequency drifts explain the width of the QPO peaks in the power spectra during the type II bursts. From an analysis of the X-ray spectrum as observed during the maxima and minima of the oscillations, we find that the oscillations can be described by changes of the temperature of a blackbody emitter of constant apparent area. We discuss the possible implications of our results for mechanisms of the different types of QPOs observed in low-mass X-ray binaries and for models of the type II bursts from the Rapid Burster.

Subject headings: stars: individual (MXB 1730–335) — stars: pulsation — X-rays: bursts

I. INTRODUCTION

During observations with the Japanese X-ray satellite *Hakucho* in 1979, Tawara *et al.* (1982) detected ~ 2 Hz pulsations in the X-ray intensity of two (out of 63) type II bursts from the "Rapid Burster" (MXB 1730–335; Lewin *et al.* 1976). The periods measured during these two bursts differed by $\sim 1\%$, and Tawara *et al.* (1982) concluded that, therefore, these pulsations do not reflect the rotation period of a neutron star.

It is possible that these ~ 2 Hz pulsations are an example of the quasi-periodic oscillations (QPOs), which have been detected since 1985 in the X-ray flux of about a dozen X-ray sources, particularly in the so-called galactic bulge X-ray sources, i.e., the luminous low-mass X-ray binaries located in the central regions of the Galaxy (see, e.g., Lewin, van Paradijs, and van der Klis 1988; van der Klis 1989; Hasinger and van der Klis 1989 for reviews of the properties of these QPO sources). From a 2-day *EXOSAT* observation of the Rapid Burster, Stella *et al.* (1988*b*) found that this remarkable X-ray

source is unique not only with respect to its burst properties, but with respect to its QPO behavior as well. It is therefore not clear that the QPOs from the Rapid Burster and those seen in other low-mass X-ray binaries are caused by the same mechanism(s).

Stella *et al.* (1988*b*) found ~ 2 –5 Hz QPOs during about half of 40 very long type II bursts; the QPO frequency was anti-correlated with the average peak flux of the bursts. QPOs were also detected during some of the intervals of persistent emission between bursts; the frequency of these persistent emission QPOs, which likewise ranged between 2 and 5 Hz, evolved generally in a highly complex manner. In a subsequent study, Stella *et al.* (1988*a*) found that in the persistent emission QPOs, the variations at low photon energies lagged those at high photon energies by ~ 7 ms, when the QPO frequency was > 3.6 Hz; no time lags were detected in the QPOs during bursts, or in the persistent emission QPOs with frequencies below 3.6 Hz.

It is unclear what determines the presence of QPOs during

bursts or persistent emission. Bursts are present in the *EXOSAT* data, which appear to be identical with respect to peak flux, total fluence, and spectral hardness, as well as time intervals since the previous burst and to the next burst; however, these bursts differ from each other with respect to the presence or absence of QPOs. A similar lack of distinction between persistent intervals with and without QPOs was found.

During an observation in 1988 August with the Japanese X-ray satellite *Ginga* of the X-ray burst source 4U/MXB 1728–34, we noted that the Rapid Burster, which was also included in the field of view, was active, and emitted type II bursts about once every ~ 15 s. We decided to terminate the observation of 4U/MXB 1728–34 and moved the satellite in order to maximize the signal from the Rapid Burster.

In this paper, we present results of an analysis of these *Ginga* data (a presentation of some of these results was given previously by Mitsuda 1988b). The observations and data analysis are outlined in § II. In § III, we describe the burst behavior and the properties of the QPOs during the bursts (no QPOs were detected in the persistent emission). In § IV, we discuss our results.

II. OBSERVATIONS

Observations of the X-ray burst source 4U/MXB 1728–34 with the large area counter (LAC) array (Turner *et al.* 1989) on *Ginga* (Makino *et al.* 1987) started on 1988 August 10, UT 23:47. This source is located at an angular distance of $25'$ from the Rapid Burster, which was therefore also included in the $1^\circ \times 2^\circ$ (FWHM) field of view of the detectors. When it was noted that the Rapid Burster was active, the satellite was pointed to a direction near this source, on August 11, UT 02:50. At this pointing position, the transmission of the signals from the Rapid Burster and 4U/MXB 1728–34 were $\sim 90\%$ and $\sim 60\%$, respectively. Between August 12, UT 06:18 and August 14, UT 23:50, the pointing position of the satellite was changed in order to exclude 4U/MXB 1728–34 from the field of view of the LAC (the transmission of the signal from the Rapid Burster was then $\sim 40\%$).

The time intervals between consecutive data links to the satellite varied between one and 10 satellite orbits (of 1.5 hr each). In view of limitations to the on-board data storage capacity, data were collected at a lower rate during the “remote orbits” than during the “contact orbits,” and the observations were therefore made with several combinations of time and spectral resolutions. The Rapid Burster was observed for a total effective time interval of ~ 21 hr (excluding periods of high particle background in the South Atlantic Anomaly, Earth occultations, etc.).

In this paper, we present an analysis of the data obtained during the “contact” orbits, whose time resolution is sufficiently high for a meaningful analysis of QPO. The effective

duration of these observations is ~ 7 hr, during which we detected a total of more than 400 type II bursts. For details about these observations, we refer to Table 1.

III. RESULTS

a) Burst and QPO Properties

In Figure 1, we show two representative stretches of the X-ray intensity curve of the Rapid Burster during our observations, which illustrate that during our *Ginga* observations, the source showed two distinct “modes” of burst activity.

On August 11, the Rapid Burster produced rapidly repeating short bursts (typical duration ~ 3 s), sometimes interspersed with a relatively long burst (duration ~ 30 s). During the “contact orbits,” we detected a total of 10 long bursts, 220 short bursts, and 215 intermediate bursts. The intervals between the short bursts were as short as ~ 15 s; after a relatively long burst, the interval to the next burst was on average ~ 150 s. These bursts therefore follow the relaxation oscillator-type relation between burst size and waiting time (until the next burst) observed previously on many occasions (see, e.g., Lewin *et al.* 1976; Marshall *et al.* 1979; Inoue *et al.* 1980; Kunieda *et al.* 1984a, b; Stella *et al.* 1988b). We note that much longer type II bursts have been observed previously from the Rapid Burster (Basinska *et al.* 1980; Inoue *et al.* 1980; Stella *et al.* 1988b).

After August 12, the bursts had an intermediate duration of ~ 10 s and came at rather regular intervals of about a minute. Both types of burst recurrence patterns have been encountered before, e.g., during the 1976 SAS 3 discovery observations (Lewin *et al.* 1976; Marshall *et al.* 1979). Following Marshall *et al.* (1979), we will refer to these two burst recurrence patterns as “mode I” (August 11), and “mode II” (after August 12), respectively.

Average values for the peak fluxes, F_{\max} , and integrated burst fluxes, E_b , of the short (~ 3 s, mode I), the intermediate (~ 10 s, mode II), and the relatively long (~ 30 s, mode I) bursts are 1.9×10^{-8} , 1.4×10^{-8} , and 3.3×10^{-8} ergs $\text{cm}^{-2} \text{s}^{-1}$, and 4.7×10^{-8} , 7.1×10^{-8} , and 4.7×10^{-7} ergs cm^{-2} , respectively. The corresponding average time intervals to the next burst are ~ 15 , ~ 80 , and 100 – 250 s, respectively.

We detected a total of 10 type I bursts during the observation of the Rapid Burster. These bursts can be distinguished from the type II bursts by their different spectral evolution (see Hoffman, Marshall and Lewin 1978) and by the fact that they do not fit in with the recurrence pattern of the type II bursts. At least four of the type I bursts were from the Rapid Burster, because they were detected when 4U/MXB 1728–34 was outside the LAC field of view.

To investigate the fast-variability behavior of the Rapid Burster, we calculated power spectra for data strings of 16 and 32 s duration using an FFT algorithm. The normalization of

TABLE 1
JOURNAL OF OBSERVATIONS

Start Time (day; UT) (1988 August)	End Time (day; UT) (1988 August)	Net Time (s)	Mode	Time Resolution (ms)	Energy Range (keV)
10; 23:47.....	11; 06:20	6616	MPC3	7.8	0.8–18
11; 23:52.....	12; 06:18	6244	PC	0.98/1.95	1.2–17.9
12; 22:20.....	13; 03:37	5464	PC	0.98/1.95	1.2–17.9
14; 22:29.....	15; 03:42	5176	MPC3	7.8	1.2–37

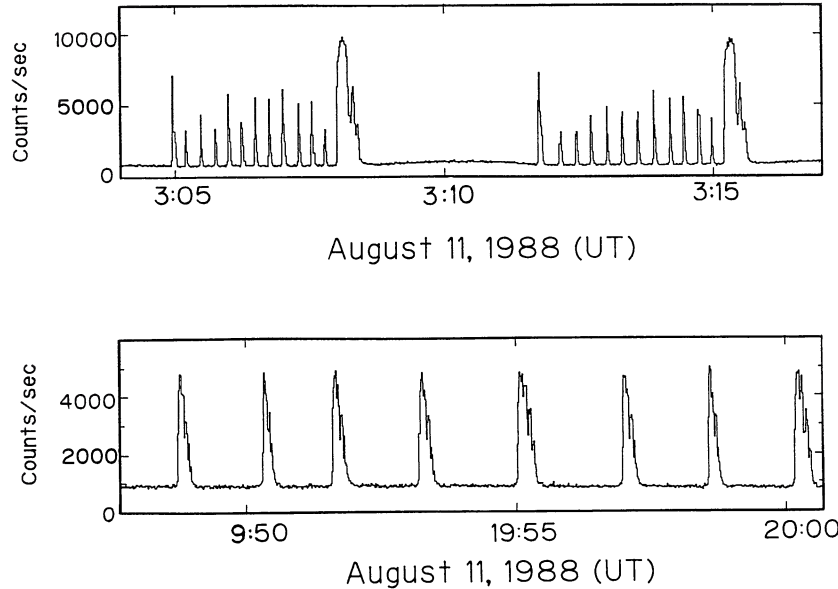


FIG. 1.—Examples of X-ray intensity curves of the Rapid Burster, in mode I (*upper panel*) and mode II (*lower panel*). These curves have been corrected for transmission efficiency, but neither the background nor the contamination from 4U/MXB 1728–34 have been subtracted.

the power spectra which we adopted is such that the fractional rms variation is given by $(P/2)^{1/2}f_m^{-1}$ (here P is the corresponding power, and f_m is the mean count rate); in other words, the power of a sine wave equals the square of the wave amplitude. The Poisson level was calculated from the probability distribution function for photon counting with dead time (for details of this timing analysis, we refer to Mitsuda and Dotani 1989).

The typical behavior of the source is illustrated in Figure 2, which shows dynamical power spectra (see van der Klis *et al.* 1985) for representative stretches of data obtained during each of the two modes of the burst activity (note that in order to illustrate possible rapid variability, the power spectra displayed in this figure are based on data strings of 2 s).

During mode I, we see QPOs in the long (30 s) bursts as regions of enhanced power near ~ 2 Hz. For the short (3 s) bursts, the presence of QPOs near this frequency is difficult to establish, because the temporal structure of the burst as a whole contributes low-frequency noise power in this very frequency region. These bursts are too short to define a smooth low-frequency noise component that could be subtracted from the power spectra. In mode II, the QPOs are present in the 10 s long bursts near ~ 5 Hz. (Some bursts of intermediate duration have power spectra that also display peaks at ~ 10 and ~ 15 Hz; an analysis of these higher frequency peaks will be described in a later paper.) During neither mode of burst activity did we find evidence for QPOs in the persistent emission.

To obtain parameters describing the QPO properties, we computed average power spectra for the long bursts and the intermediate bursts, and also, for comparison, for the persistent emission. For each intermediate burst, we selected a 16 s data set, which started 1 s before burst onset. We defined the onset time of the burst as the 0.5 s time bin in which the count rate is more than 5σ in excess of the mean value for the previous 5 s of data. The 16 s interval is long enough to cover the burst peak, where the QPOs are strongest, and does not include much “contamination” from time bins without burst emission. The power spectra of the 16 s intervals (their total number is 179) were added to obtain a mean power spectrum

for the intermediate bursts. For the long bursts, we calculated and added power spectra for data sets of 32 s, selected in a similar way (a total of nine power spectra were averaged). The average power spectra for the long and intermediate bursts are shown in Figure 3.

We calculated an average power spectrum for the persistent emission using 180 data stretches of 16 s each during the quiescent intervals following the intermediate bursts; the bursts were assumed to have terminated 5 s after the intensity had returned to within 4σ of the average preburst level.

The average power spectra were fitted with a function in which the QPOs are described with a Lorentzian peak with centroid frequency ν_{QPO} , and full width at half maximum λ , which is superposed on a power-law low-frequency component, with exponent α :

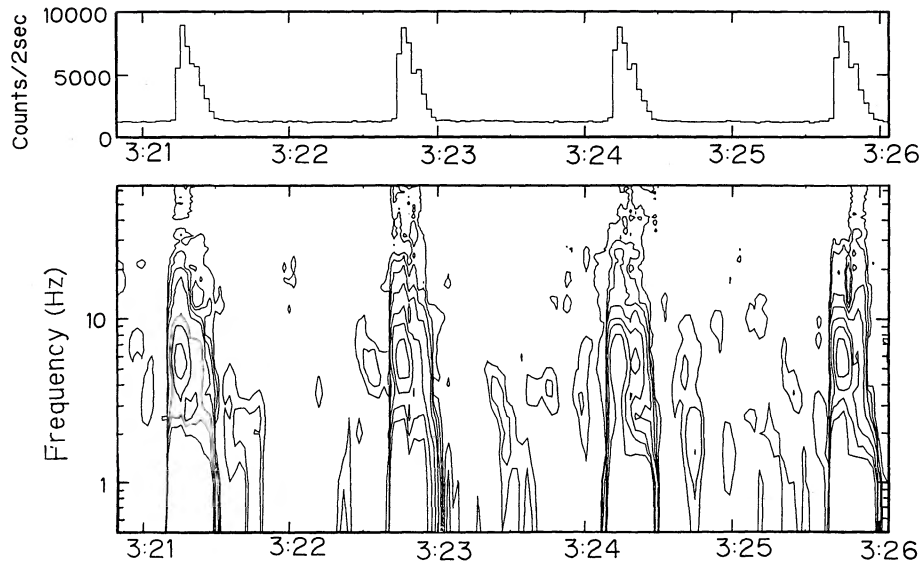
$$P(\nu) = A + B\nu^{-\alpha} + C[(\nu - \nu_{\text{QPO}})^2 + (\lambda/2)^2]^{-1}$$

(To fit the average power spectrum of the intermediate bursts, we added a second power-law component that becomes important at high frequencies; see Fig. 3).

The results of these fits are listed in Table 2 (all errors quoted correspond to 90% confidence limits). The component that rises steeply toward lower frequencies arises from the temporal structure of the bursts. We examined the effect of this burst

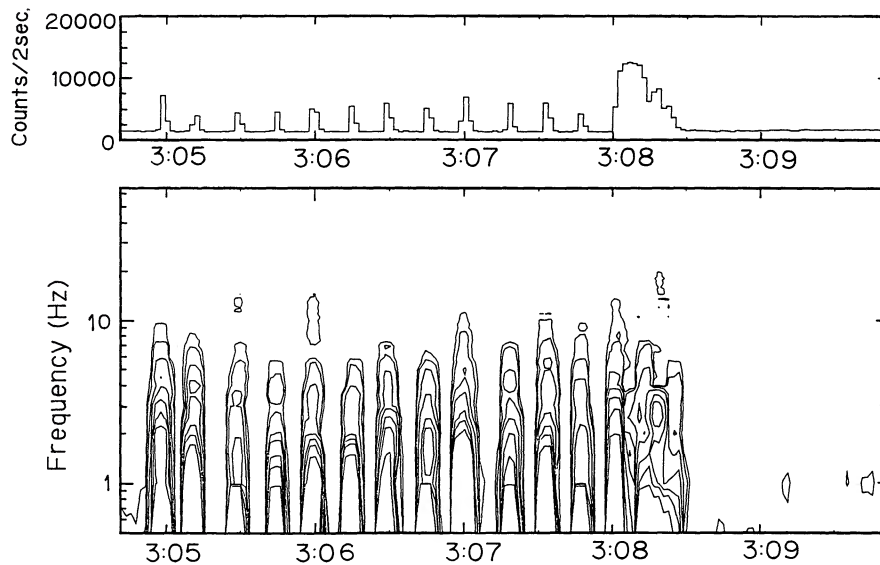
TABLE 2
PARAMETERS OF THE POWER SPECTRA

Spectra	Intermediate Bursts	Long Bursts	Persistent Emission
Red Noise:			
Power law 1 index	2.40 ± 0.07	2.5 ± 0.2	0.8 ± 0.3
Power law 2 index	0.77 ± 0.14
QPO:			
Relative amplitude (%)	19.7 ± 0.6	2.8 ± 0.5	<9.0
Frequency (Hz)	5.48 ± 0.06	2.8 ± 0.1	(5.5)
FWHM (Hz)	1.8 ± 0.2	0.7 ± 0.4	(1.8)



August 12, 1988 (UT)

FIG. 2a



August 11, 1988 (UT)

FIG. 2b

FIG. 2.—Dynamic power spectra of the Rapid Burster in (a) mode I, and (b) mode II. Upper panel shows the time variation of the X-ray intensity, lower panel shows the time variation of the power spectrum using a contour representation. In mode I, long sequences of very short bursts were interrupted by long bursts; QPOs with centroid frequency ~ 2 Hz were found in these long bursts. In mode II, the Rapid Burster emitted intermediate bursts (duration ~ 10 s) in which QPOs with frequency ~ 5 Hz were present.

profile on the QPO parameters by subtracting variations on time scales longer than ~ 1 s with a third-order spline function. The power spectra for these corrected data have the same QPO profiles, and the fitted QPO parameters are consistent with those obtained for data that were not corrected. The average power spectrum for the persistent emission showed no evidence for QPOs; the upper limit (90% confidence level) of their rms relative amplitude is 9.0%. However, we cannot yet exclude that QPOs are present during a small number of short intervals of persistent emission.

b) Burst Profile and QPOs

The decay part of type II bursts was found by Kawai (1985) and Tawara *et al.* (1985) to show a succession of peaks which are approximately the same for all bursts, except that the time scale is different. If the time scale is adjusted to the time interval, τ_c , between the first and second peaks in the burst, the burst profiles have very similar structure. (Note that following Tawara *et al.*, we counted the initial peak in the burst as the zeroth peak, etc.) Thus, with respect to stretching and shrink-

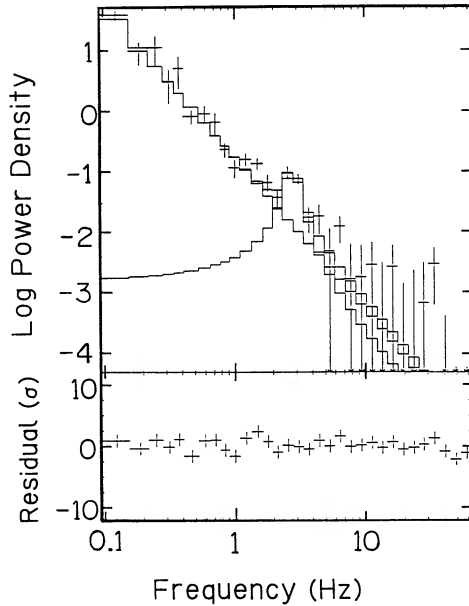


FIG. 3a

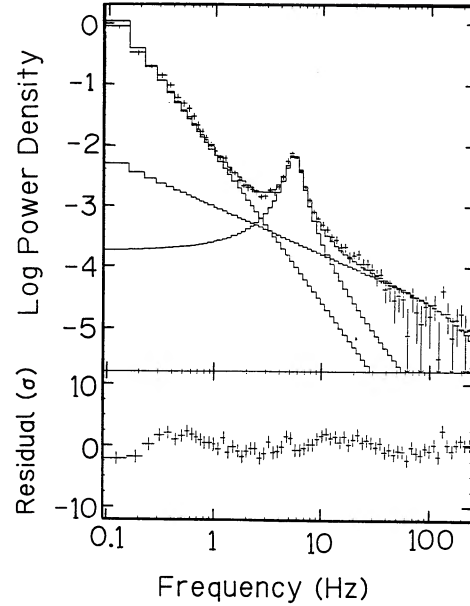


FIG. 3b

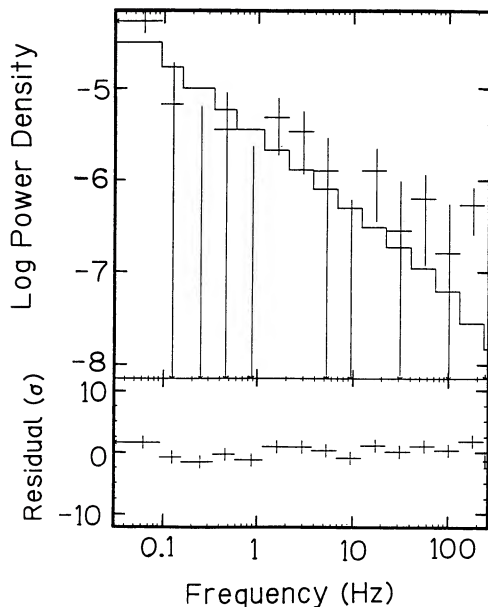


FIG. 3c

FIG. 3.—Average power spectra of the intensity variations during (a) long bursts (duration ~ 30 s), (b) intermediate bursts (duration ~ 10 s), and (c) the persistent emission between bursts. The latter data are not contaminated by a signal from the nearby source 4U/MXB 1728–34, but those for the bursts are. However, the power spectrum of 4U/MXB 1728–34, based on data obtained on 1988 August 24, when the Rapid Burster was not active, did not show QPO structure.

ing of the time axis, the burst profile behaves like an accordion. Kawai (1985) and Tawara *et al.* (1985) called this the time scale-invariant burst profile. They found that this invariance holds for bursts with characteristic time scales τ_c ranging over a factor 30, between 0.3 and 9 s. Tawara *et al.* (1985) also found that the successive peak positions are phased in such a way that the intervals between the even-numbered peaks and, independently, those between the odd-numbered peaks, compose

geometric series with the same multiplication factor 0.57 (i.e. the time intervals between the peaks decrease as the burst progresses). The odd-numbered peaks fall approximately halfway between the even-numbered ones. Tawara *et al.* (1985) also found evidence that during the odd-numbered peaks, the X-ray spectrum is somewhat harder than during the even-numbered peaks.

A very remarkable property of the 5 Hz QPOs is that their presence seems to be related to the time scale-invariant profile (see Fig. 4). They generally appear very strongly during the zeroth peak and become much weaker before the end of this peak; they are not seen clearly during the first peak, and reappear again strongly at the onset of the second peak. The statistical quality of the data is insufficient to identify the QPOs in the third (and possibly later) peaks. We have calculated the power spectra for each peak in five bursts that showed a clear time scale-invariant profile. In Figure 5, we show the average power spectra of the first three peaks of the five selected bursts. The relative amplitudes of the QPOs are $20.2 \pm 1.8\%$ (zeroth peak), less than 2.2% (first peak), and $15.3 \pm 2.1\%$ (second peak). Here the errors and upper limit correspond to 90% confidence levels. In addition, the X-ray spectrum appears to be harder during the even-numbered peaks than during the odd-numbered peaks. Hence, some mechanism appears to exist in the Rapid Burster that distinguishes the even- and odd-numbered peaks. This suggests that perhaps the time scale-invariant profile and the QPOs have a related origin. This point is discussed further in § IV.

c) Individual Oscillations

One of the characteristics of the QPOs from the Rapid Burster, which will turn out to be important for the present investigation, is their large relative amplitude. As a result of this, the individual oscillations are directly visible in the X-ray intensity curve, as is clear from Figure 4, in which the count rate history is shown, at several time scales, for three bursts of intermediate duration. Previously, a glimpse of individual oscillations in type II bursts from the Rapid Burster was seen in *EXOSAT* data (Stella 1988). In some bursts, the QPOs

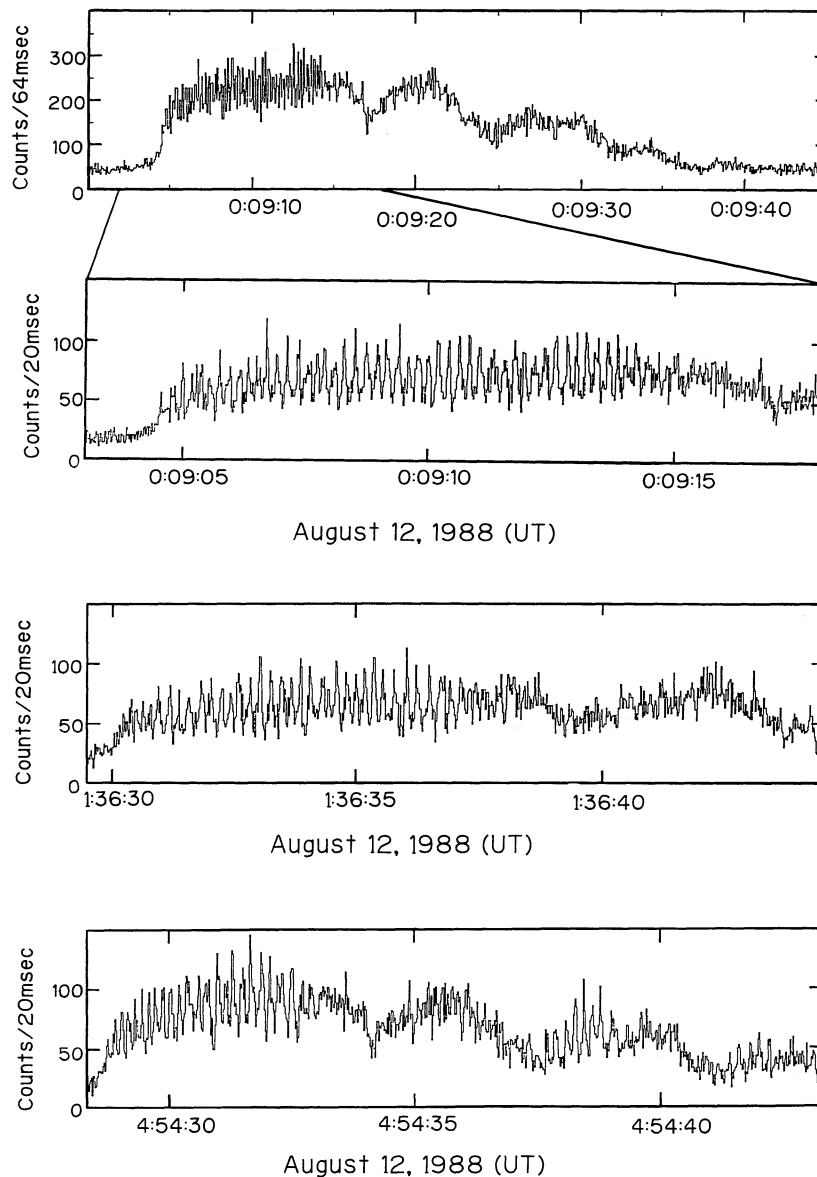


FIG. 4.—Count rate history for three intermediate bursts from the Rapid Burster (data not corrected for transmission efficiency). The individual oscillations of the ~ 5 Hz QPOs are clearly seen during the first and third peaks of the bursts.

clearly appear already just after onset of these bursts when they are on the initial rise to burst maximum. The amplitudes of the ~ 2 Hz QPOs in the long bursts are much smaller than those of the ~ 5 Hz QPOs in the intermediate bursts (see Table 2; this agrees with the results of Stella *et al.* 1988*b*). As a result of this, the individual ~ 2 Hz oscillations are not clearly visible in the X-ray intensity curve. For this reason, we report here on the QPOs in the intermediate bursts only.

For ~ 60 intermediate bursts, in which individual oscillations could be clearly seen in the X-ray intensity curve, we have measured the times of the maxima in series of consecutive ~ 5 Hz oscillations, whenever the statistical quality of the data allowed us to ensure that no maxima were missed. For most of such uninterrupted series of oscillations, observed during the initial (zeroth) peak in the burst, we find that the times of maximum intensity show a characteristic pattern. The difference between the observed time of maximum intensity (O) and

the calculated time (C), expected for a coherent oscillation with the average frequency of the oscillation, often initially decreases, and then increases (see Fig. 6 for a few examples). The rather smooth upward curvature of these O–C plots indicates that for these bursts, the decrease of the oscillation frequency is continuous throughout the series of oscillations. For about one-quarter of the bursts, the O–C behavior is more complicated (some examples are shown in Fig. 6). In particular, we find in a number of bursts that the frequency decrease stops and turns into a frequency increase. In one case, we find an approximately sinusoidal variation of the frequency with a period of the order of ~ 10 oscillations. However, also in these cases, the O–C curve is generally smooth. The rms scatter of the individual times of maximum intensity with respect to the smoothed O–C curve is typically less than 0.15 cycles.

Thus, the behavior of the QPO during the initial peak of the burst is that of an oscillator whose frequency, at each instant, is

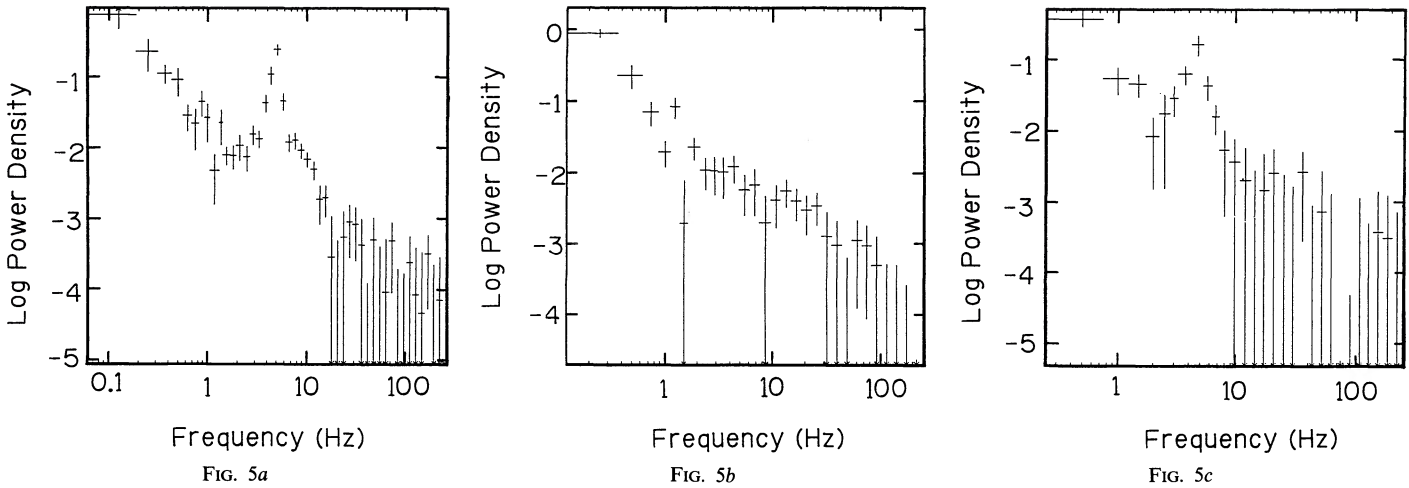


FIG. 5.—Averaged power spectra for the (a) zeroth, (b) first, and (c) second peaks of five bursts from the Rapid Burster, which showed the time-invariant structure. QPOs are present during the first and third peaks but are conspicuously absent during the second peak.

well determined but changes gradually by a significant amount over a time interval corresponding to ~ 20 – 40 cycles. In $\sim 75\%$ of the bursts, the frequency change is a decrease, but in others we observed both a decrease and an increase of the frequency.

To describe the average frequency behavior in these QPOs we have for each burst determined the average frequencies, ν_1

and ν_2 , during the first five and the last five cycles during the above uninterrupted sequences of oscillations, respectively. Their average values are $\nu_1 = 6.2 \pm 0.9$ (0.12) Hz, and $\nu_2 = 5.2 \pm 0.6$ (0.07) Hz, respectively. The errors are one standard deviation of the distribution of values for individual bursts and the mean error of this distribution (in parentheses), respectively. The average value of the frequency ratio, measured for individ-

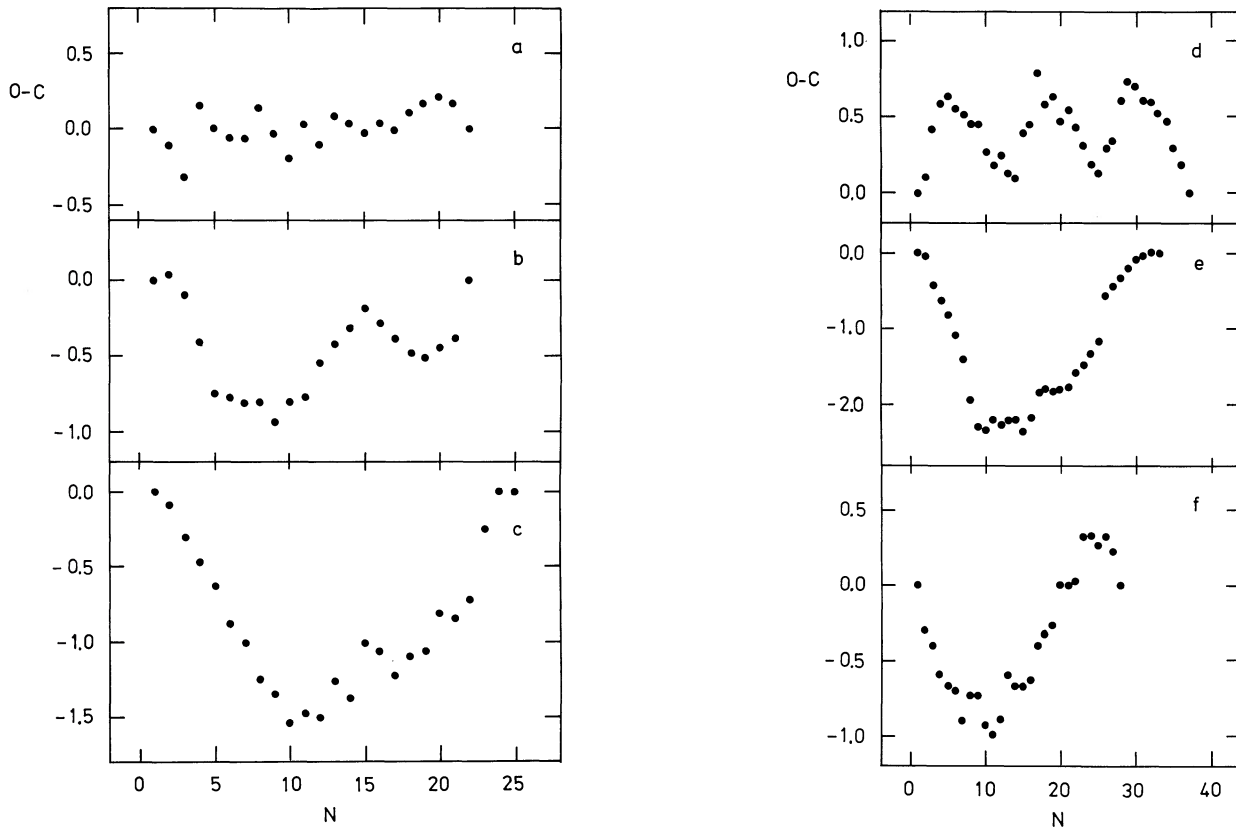


FIG. 6.—Difference (in units of cycles) between the observed time (O) of maximum intensity during individual ~ 5 Hz oscillations, and the time (C) calculated for a coherent oscillation with the mean oscillation frequency, plotted as a function of oscillation number. Upward curvature of the (O–C) curve indicates a decrease of the oscillation frequency. During most bursts, the frequency decreases (e.g., c, e, f), but more complicated frequency changes have been observed (e.g., b, d). The scatter around smooth interpolated (O–C) curves corresponds to an rms phase jitter which is generally less than 0.15 cycles.

ual bursts, equals 1.23 ± 0.17 (0.023). Thus, the decrease of the frequency of the oscillations during the zeroth peak of the type II bursts is typically 20%–25%; this frequency change accounts for the width of the QPO peaks in power spectra for data trains that cover the whole initial peak of the bursts.

With few exceptions, the data during the second peak of the bursts do not allow a detailed study of a frequency drift of the oscillations (where this was possible, the oscillations likewise showed a frequency drift). The frequency, ν_3 , of these oscillations is, on average, somewhat smaller than ν_2 (see above). The average of the ratio ν_2/ν_3 equals 1.09 ± 0.16 (0.025).

Although in the bursts that we have studied in detail, the frequency generally decreases during the zeroth peak, and from the zeroth to the second peak, a continuous frequency decrease does not occur during all type II bursts. Stella *et al.* (1988*b*) observed rather small variations in the frequency of QPOs in bursts (averaged over ~ 16 s), but these variations did not show systematic trends during the bursts (which lasted between ~ 100 and ~ 600 s). Also, the frequency variations observed by Tawara *et al.* (1982) in the ~ 2 Hz pulsations they detected, which occurred on time scales of about half a minute, are quite small (a few percent) compared to the changes we have observed. Although it is possible that the frequency decrease which we have found during most type II bursts is typical for the particular episode of burst activity we observed, it appears more likely that this frequency decrease normally occurs early in the burst, but that on time scales longer than ~ 10 s, there is very little net frequency variation.

d) Photon Energy Dependence of the QPOs

We have investigated the photon energy dependence of the ~ 5 Hz QPOs by making average power spectra, separately, for seven different photon energy channels covering the energy range 1.2–18.5 keV, using the 16 s data sets that start 1 s before the onset of the intermediate bursts. The temporal structure of the burst on a time scale greater than 1 s has not been subtracted from the data because, as mentioned above, they have little effect on the QPO properties. We fitted a power law plus a Lorentzian peak to the power spectrum of each energy channel in order to estimate the QPO parameters. We restricted these fits to frequencies above 1 Hz. The results are listed in Table 3. It appears that for the ~ 5 Hz QPOs, the QPO frequency, within the accuracy of its determination, is independent of the photon energy band; the relative QPO amplitude increases with photon energy (see Fig. 7).

This hard relative QPO spectrum is not inconsistent with either the hard relative spectra reported for horizontal branch

TABLE 3
PHOTON ENERGY DEPENDENCE OF THE ~ 5 Hz QPO

Energy (keV)	Relative Amplitude (%)	Centroid Frequency (Hz)	Time Lag (ms)
1.2–2.2	< 10.6	(5.5)	-3.8 ± 5.1
2.2–4.5	7.5 ± 0.8	5.0 ± 0.3	Reference
4.5–6.8	11.8 ± 0.8	5.5 ± 0.2	-0.2 ± 1.4
6.8–9.2	11.9 ± 1.3	5.5 ± 0.3	0.1 ± 1.7
9.2–11.5	13.8 ± 2.0	4.7 ± 0.3	-1.1 ± 2.6
11.5–13.8	14.1 ± 3.6	5.4 ± 0.7	-2.1 ± 3.8
13.8–18.5	< 16.0	(5.5)	2.6 ± 4.7

NOTE.—Positive time lag means that the variations lag those in the reference channel. The FWHM of the QPO has been fixed at 1.76 Hz.

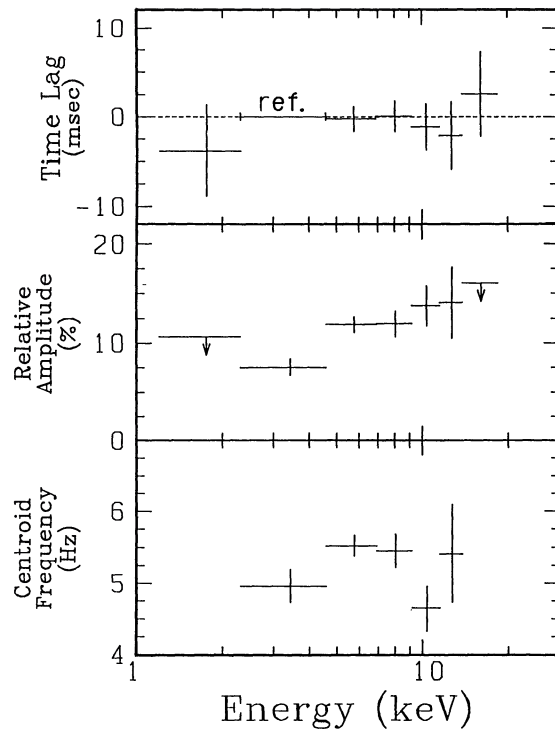


FIG. 7.—Photon energy dependence of the centroid frequency, the amplitude, and the time lag (measured relative to the energy channel near ~ 3 keV) in the ~ 5 Hz QPO observed in type II bursts, of intermediate duration, from the Rapid Burster. No significant dependence of either the centroid QPO frequency, or the relative time lag, is present. The relative amplitude of the QPO shows a moderate increase with energy, from $\sim 7\%$ near 3 keV, to $\sim 14\%$ near 12 keV.

QPOs (van der Klis 1986; Mitsuda 1988*b*), or the more complex relative spectrum of the normal branch QPOs in Cyg X-2 (Mitsuda 1988*a*).

From the same data that we used to investigate the energy dependence of the QPOs we have calculated the cross-correlation functions (CCFs) between the variations in the different energy bands. However, for this purpose we first subtracted burst temporal structure on time scales in excess of 1 s from the data, using a third-order spline function. We described the CCF (using a model that is appropriate for an oscillating-shot model for the QPO) by using the following expression:

$$CCF(s) = \{C_{RN} + C_{QPO} \cos [2\pi\nu(s - s_0)]\} \exp(-|s - s_0|/\tau).$$

Here s is the time lag variable and s_0 can be interpreted as the average time lag between the high-energy and the low-energy photons.

The results of fitting the CCF with this model are listed in Table 3, and s_0 is plotted as a function of photon energy in Figure 7. Our results indicate that no significant time lags occur between the intensity variations in different photon energy ranges, with upper limits (90% confidence level) between ~ 2 and ~ 5 ms, which is consistent with the findings of Stella *et al.* (1988*b*).

e) Temperature Oscillations

Since the QPOs from the Rapid Burster are visible in the X-ray intensity curve, we can investigate their energy spectra directly. In an attempt to identify the parameters which cause

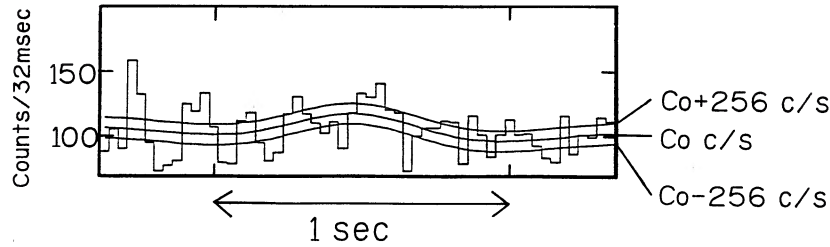


FIG. 8.—Illustration of the method employed to calculate the X-ray spectrum during the peak and the valley of the QPO. The middle curve, labeled C_0 , is the smoothed time variation of the count rate. The data for which the count rates are larger than $C_0 + 256 \text{ c s}^{-1}$ and smaller than $C_0 - 256 \text{ c s}^{-1}$, have been used to obtain the X-ray spectrum during the maximum and minimum intensity, respectively.

the oscillations, we have calculated the energy spectra around the peaks and the valleys of the QPOs. To obtain these spectra, we have used the following procedure: (i) we first calculated the smoothed burst profile, $C_0(t)$, which contains only variations on a time scale longer than $\sim 1 \text{ s}$, using a third-order spline function; (ii) we selected data (every 32 ms) whose count rate is larger (smaller) than the smoothed burst profile by δC_0 counts s^{-1} (see Fig. 8). Since δC_0 should be larger than the Poisson fluctuations, we have adopted for δC_0 values of 128 or 256 c s^{-1} , depending on the observed burst flux; (iii) from the data selected accordingly, the persistent emission was subtracted. The resulting energy spectra correspond to those at the maximum and minimum of the QPOs.

The energy spectrum of the type II bursts can be reasonably well described by that of a blackbody whose temperature does not change much during the bursts (see, e.g., Marshall *et al.* 1979; Kunieda *et al.* 1984a). However, some deviations have appeared in recent high-sensitivity observations (Kawai 1985; Stella *et al.* 1988b). Stella *et al.* (1988b) found that a blackbody did not represent well the 2–15 keV burst spectra, but that an unsaturated Comptonization spectrum provided an acceptable fit. Kawai (1985; see also Kawai *et al.* 1988) pointed out that the type II burst spectra show some excess emission above a

blackbody curve at energies above $\sim 10 \text{ keV}$, which can be fitted if Comptonization of the blackbody emission by a hot plasma is taken into account (see Nishimura, Mitsuda, and Itoh 1986). We have adopted here a Comptonized blackbody spectrum as a model for the energy spectra in the peaks and valleys of the QPOs. We fixed the low-energy absorption column density ($N_{\text{H}} \text{ cm}^{-2}$) to the mean value ($\log N_{\text{H}} = 22.0$) during the bursts, because the data have an energy binning that is too coarse to determine the column density unambiguously. We also fixed the temperature of the Comptonizing plasma to 100 keV, because the electron temperature and the Compton scattering optical depth are strongly correlated in the fit and difficult to determine independently (see Mitsuda *et al.* 1989). The normalization of the Comptonized blackbody is defined to be proportional to the area of the blackbody emitter but independent of its temperature.

The energy spectra observed during maxima and minima of the individual oscillations, together with their best-fit model functions, are shown in Figure 9; the best-fit parameters are listed in Table 4. In Figure 10, we show a χ^2 contour map, between the normalization and the temperature of the Comptonized blackbody, which shows that the temperature difference between the QPO spectra at maximum and minimum is

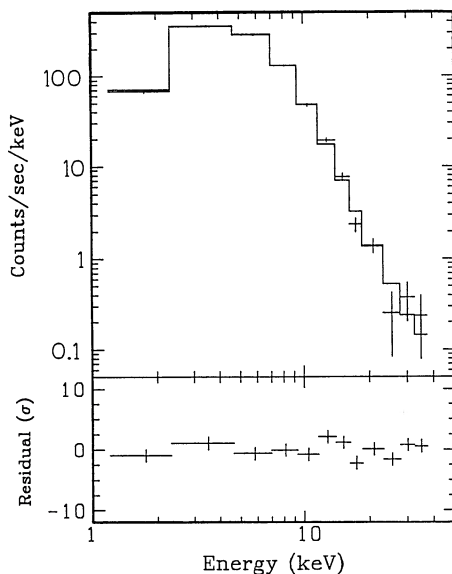


FIG. 9a

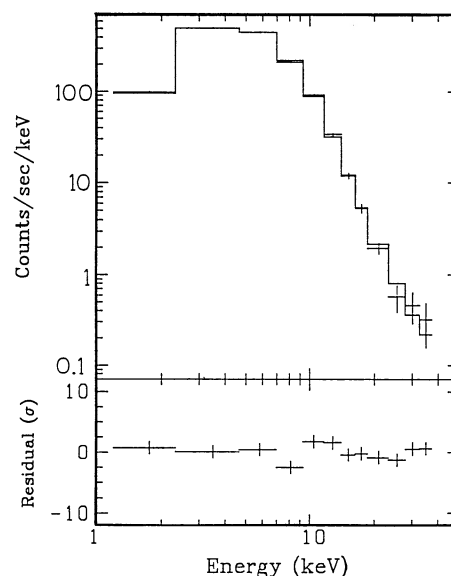


FIG. 9b

FIG. 9.—X-ray spectra obtained during (a) the valley and (b) the peak of the QPO, using the method illustrated in Fig. 8. The model function used in the spectral fitting is a Comptonized blackbody spectrum which is almost the same as a blackbody below $\sim 10 \text{ keV}$, but which has a noticeable hard tail. Within the framework of a Comptonized blackbody spectral model the difference between these two spectra, shown here, is caused mainly by a change of the temperature of the Comptonized blackbody.

TABLE 4
ENERGY SPECTRA AT MAXIMUM AND MINIMUM INTENSITY IN THE ~ 5 Hz
QPO

INTENSITY	COMPTONIZED BLACKBODY		
	Normalization	Temperature (keV)	Optical Depth
Maximum	856 ± 60	1.52 ± 0.02	0.26 ± 0.03
Minimum	770 ± 65	1.40 ± 0.03	0.28 ± 0.03

significant, whereas there is no difference in their normalizations. The results of the spectral fits show that the optical depth and the normalization of the Comptonized blackbody are the same within the errors for the QPO peak and valley spectra.

A general problem with analytic fits to observed spectra of the type we have made is the difficulty to prove their uniqueness, so usually one needs a good physical *a priori* reason for adopting a particular functional form. If, nonetheless, we take the above result at face value, it implies that the QPOs during the type II bursts are generated mainly by changes of the blackbody temperature and not of the apparent size of the emitter. This result is not inconsistent with the absence of a significant time lag between the intensity variations at different photon energies, if the oscillations are symmetric. Variations of the emitting area, at a constant blackbody temperature, never produce time lags; however, such variations do not explain the energy dependence of the QPO amplitude (see above).

IV. DISCUSSION

a) QPOs in Type II Bursts

During our observations, the Rapid Burster showed QPOs, with centroid frequencies, ν_{QPO} , near 5 Hz, and near 2 Hz, in all bursts which lasted for ~ 10 and ~ 30 s, respectively. The QPOs observed previously by Tawara *et al.* (1982) in 2 (out of

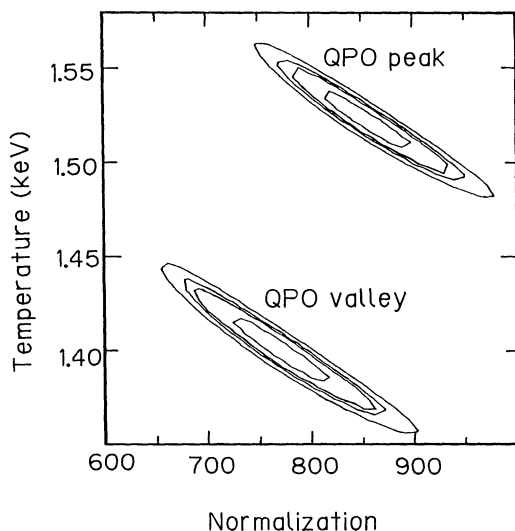


FIG. 10.— χ^2 contours in a diagram of temperature vs. normalization of the Comptonized blackbody spectrum, corresponding to the X-ray spectra during the QPO peak and valley. The contours indicate 60%, 90%, 95% and 99% levels of confidence. The difference between the two temperatures is significant, whereas the normalization, which is proportional to the area of the emitting region but is independent of the temperature, is not significantly different for the two spectra.

63) bursts had a frequency of 2 Hz; those observed by Stella *et al.* (1988b) in 23 (out of 40) bursts, and in the persistent emission, almost invariably had frequencies in the 2–5 Hz range. Thus it appears that the 2–5 Hz frequency range is favored by the QPOs from the Rapid Burster (note, however, that on a number of occasions, Stella *et al.* also observed QPOs below ~ 1 Hz in the persistent emission just before the onset of type II bursts).

Stella *et al.* (1988b) found that the centroid frequency of QPOs during bursts is strongly anticorrelated with the average peak flux, F_{max} , of the bursts and shows a positive correlation with their effective duration (defined as the ratio $\tau = E_p/F_{\text{max}}$), which ranges between ~ 75 and ~ 650 s. The QPO frequencies during the type II bursts observed by Tawara *et al.* (1982), and by us (see Table 2), fit the former relation reasonably well. However, we find that in our data the QPO frequency is anticorrelated with the effective burst duration (ranging from ~ 10 to ~ 30 s). Thus, there does not appear to exist a monotonic (ν_0, τ) relation extending beyond $\tau \sim 30$ s. This is likely the result of a nonmonotonic relation between burst peak flux, and burst duration (see Kunieda *et al.* 1984a; Basinska *et al.* 1980).

From our analysis of the times of the maxima of the individual 5 Hz oscillations in uninterrupted wave trains, we have found that at each instant of time, the oscillations are periodic (they “know” what their frequency is: the rms phase jitter of the times of maximum intensity is less than 0.15 cycles). However, their frequency changes by up to $\sim 25\%$ during the burst. Most bursts that we have analyzed show a frequency decrease during the first peak of the burst, but a fair number of examples have been found in which the frequency increases or in which the frequency both decreases and increases (see Fig. 6).

During some previous observations of the Rapid Burster, type II bursts have been observed which lasted much longer (up to > 10 minutes) than observed by us with *Ginga* (see, e.g., Basinska *et al.* 1980; Inoue *et al.* 1980; Tawara *et al.* 1982; Stella *et al.* 1988b). The QPO centroid frequencies, as determined from data stretches of generally more than 10 s duration, remained approximately constant during these long bursts (Tawara *et al.* 1982; Stella *et al.* 1988b). This may indicate that during such long bursts, the frequency of the oscillations varies on a time scale of less than ~ 10 s over a limited range around an average value. It might be this frequency drift which accounts for the width of the QPO peaks in power spectra obtained during type II bursts from the Rapid Burster.

It has been noted before (Stella *et al.* 1988b) that the Rapid Burster lacks the strong QPO-related low-frequency noise that is typical of horizontal branch QPOs. Our data are consistent with this: the red noise visible in Figure 3 is nearly entirely caused by the overall variation in the type II bursts (in particular, the burst onset). This property of the power spectrum of the Rapid Burster is hard to reconcile with models where the QPOs are caused by oscillating shots, and it is in direct contradiction with models where the shots are positive-definite. The frequency drift of the oscillations reported here provides a natural explanation for the lack of low-frequency noise and the width of the observed QPO peaks in the power spectrum, without requiring amplitude-modulated oscillating shots that are fine-tuned to suppress low-frequency noise.

Another consequence of the visibility of individual 5 Hz oscillations in the X-ray light curve is that this allowed us to study the X-ray spectrum as a function of phase (maximum

and minimum intensity) in the oscillations (see § IIIe). We found that within the framework of a specific spectral model, the oscillations are predominantly a result of (blackbody) temperature variations, with the area of the blackbody emitter remaining approximately constant (for an assumed distance of 10 kpc, the corresponding blackbody radii during the maximum and minima of the oscillations are 14.4 ± 1.0 and 13.8 ± 1.2 km, respectively, similar to values previously found; see, e.g., Marshall *et al.* 1979; Kawai 1985). Although, as yet, it is hard to exclude other causes for the QPOs seen in the Rapid Burster, this result suggests that they might be caused by variations in the accretion rate, which are transformed into variations in the emitted radiative power on a time scale which is very short compared to the period of the QPO (i.e., substantially less than $\sim 10^{-1}$ s).

Temperature changes were also found by Kawai (1985) in the intensity variations of the time-invariant structure of type II bursts observed with *Tenma*, which however occur on time scales of order seconds. However, no clear evidence for such temperature variations were found in a similar time-resolved spectral analysis of type II bursts observed with *EXOSAT* (Tan *et al.* 1989). Thus, the spectral variations in the QPO and in the time scale-invariant burst profile do not support the idea that the time scale-invariant structure is a very low-frequency extension of the QPO. Further arguments for this conclusion are: (i) the proportionality between QPO period and burst duration, which holds for the bursts we observed, does not extend to the very long bursts observed by Stella *et al.* (1988b); (ii) the spectral analogy cannot be carried over to time scales as long as the duration of the bursts, because the overall intensity variation in the type II bursts is mainly a result of a variation in apparent radius of a blackbody emitter at an approximately constant temperature (Hoffman, Marshall, and Lewin 1978; Marshall *et al.* 1979; Kawai 1985), and not by blackbody temperature variations.

In principle, there are various ways in which a quasi-periodic signal can be generated, e.g., by a superposition of randomly excited damped harmonic oscillators, by random phase variations in a periodic wave train, or by frequency variations on a time scale that is shorter than the length of the data stretches for which individual power spectra are made. We have shown that for the QPOs during the type II bursts from the Rapid Burster, the latter is the case; i.e., the frequency drift causes the oscillations to appear as quasi-periodic.

Although, in view of the unique burst properties of the Rapid Burster, it might be argued that also the oscillations in this source are of a very special kind, it is likely that frequency drift also provides the underlying model for at least some of the QPOs observed in other low-mass X-ray binaries: in at least one other case, GX 339-4, *Ginga* data have shown that ~ 6 Hz QPOs are likewise caused by relatively slow frequency drift of an oscillation that at each point of time is coherent (Dotani 1989).

b) Comparison with QPOs in Other Sources

In considering the applicability of our results to the QPOs observed in other low-mass X-ray binaries, we have made a distinction between various types of QPOs that have been observed in these sources, based on the recent classification of low-mass X-ray binaries (LMXBs) proposed by Hasinger and van der Klis (1989). These authors propose that, based on the combined X-ray spectral and fast-variability characteristics,

two types of LMXBs can be distinguished, which they call the “Z sources” and the “atoll sources.”

The Z sources show a characteristic pattern of three connected “branches” in an X-ray color-color diagram, which are called the horizontal, normal, and flaring branches, respectively. While on the horizontal branch (HB), the sources exhibit ~ 20 – 50 Hz QPOs, with a strong correlation between frequency and source intensity; these HB QPOs are accompanied by an approximately equally strong “low-frequency noise component.” In the normal branch (NB), these two components are much weaker in the power spectrum; instead, it shows a QPO peak at an approximately constant frequency (in a number of cases slightly anticorrelated with source intensity), which for all sources is located near ~ 6 Hz. In a few sources, QPOs have been observed in the flaring branch (FB), with properties that join smoothly to those observed on the NB. As the source moves upward along the FB, the QPO peak broadens and merges into a very broad high-frequency noise component. In all branches, a very low frequency noise (VLFN) component is present in the power spectra, which can be adequately described as a rather steep power law in frequency; this VLFN generally dominates the power spectrum below ~ 0.1 Hz. The QPO properties change discontinuously as the source moves from the HB to the NB; between the NB and the FB, the change in QPO properties is gradual. This has been interpreted as evidence for the existence of two different QPO mechanisms. Gated accretion according to magnetospheric beat-frequency models (Alpar and Shaham 1985; Lamb *et al.* 1985) provides a good description of the HB QPOs. It has recently been proposed that the NB/FB QPOs are related to disturbances in a radiation-dominated plasma at a near-Eddington limited accretion rate, in which the relevant propagation speed of the disturbances is the speed of sound (Hasinger 1987; Lamb 1990).

The X-ray color-color diagrams for the atoll sources do not show the above-described characteristic Z pattern; instead, they display a “banana branch” and isolated “islands,” which together form an atoll-like configuration. In the banana branch, the power spectra are dominated by a power-law VLFN component; the island state is correlated with power spectra that are dominated by a strong high-frequency noise component, which in some cases looks like a very broad QPO peak (see Hasinger and van der Klis 1989 for details).

Even a superficial comparison of the HB QPOs with the QPOs observed from the Rapid Burster shows that they are very different. Their frequency ranges are generally between ~ 20 and ~ 50 Hz, and below ~ 5 Hz, respectively. The HB QPOs show a strong positive correlation with source intensity, whereas presently available data indicate an anticorrelation for the Rapid Burster. Also, the power spectrum for the Rapid Burster does not show the strong LFN component observed during the HB. Independent of this comparison of observable quantities, we note that it seems hard for beat-frequency models (Alpar and Shaham 1985; Lamb *et al.* 1985) to account in a natural way for the fact that the quasi-periodic nature of the oscillations is a result of slow frequency drifts of a long uninterrupted train of oscillations.

The power spectra of the atoll sources and the Rapid Burster have the presence of a power-law VLFN component, and the absence of LFN, in common; however, the rather narrow QPO peak found for the Rapid Burster is very different from the HFN component observed in the power spectra of atoll sources.

As suggested previously by Stella (1988), the power spectra for the Rapid Burster appear to be somewhat similar to those observed during the NB spectral state of the Z sources. In the first place, although the Rapid Burster shows larger frequency variations than each of the individual Z sources, the observed ranges in QPO frequency are not much different (generally ~ 2 – 5 Hz for the Rapid Burster and ~ 5 – 7 Hz for the NB QPOs). Secondly, the power spectra have in common the presence of a power-law VLFN component and the absence of the strong LFN component (as observed in the HB power spectra). Also, in a number of cases, a weak anticorrelation has been observed between the NB QPO frequency and the source intensity (see, e.g., Middleditch and Priedhorsky 1986), which agrees, at least in a qualitative sense, with the results observed for the Rapid Burster. Finally, both the NB QPOs and the QPOs from the Rapid Burster show an increase in relative amplitude toward higher photon energies in the 5–20 keV range (Hasinger 1986; Mitsuda 1988a; Mitsuda and Dotani 1989).

These results show that, at least on a phenomenological level, the QPOs observed in the type II bursts from the Rapid Burster appear to be quite similar to those observed during the NB state of Z sources (see Fig. 11). This raises the possibility that the latter are also the result of continuous oscillations, which at each moment are periodic, but whose frequency drifts.

Following a qualitative scenario by Hasinger (1987), Lamb (1990) recently proposed a model for the normal branch QPOs, in which these reflect variations of the accretion rate related to disturbances propagating at the sound speed in a radiation-dominated flow near the Eddington limit. In view of the large range in peak burst flux, at which the 2–5 Hz QPOs from the Rapid Burster have been observed, it is unlikely that the mechanism that produces them is related to processes occurring near the Eddington limit. Therefore, if the QPOs in the Rapid Burster and the NB QPOs are produced by the same mechanism, this mechanism is probably a different one from that proposed by Lamb (1990).

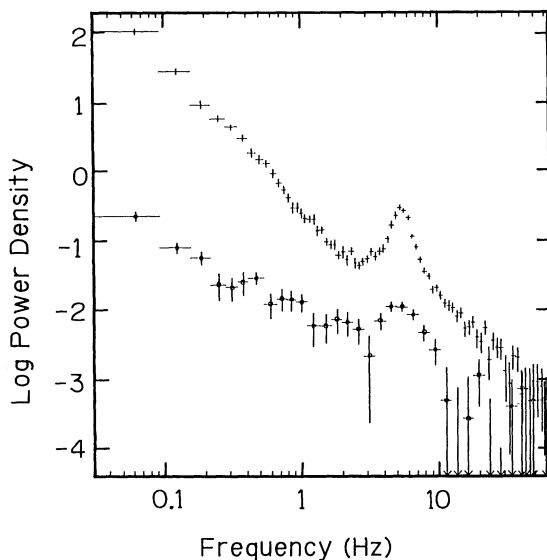


FIG. 11.—Power spectrum of one day of data of the Rapid Burster, compared to that of the Z-type source Cyg X-2 (Mitsuda and Dotani 1989) during its normal branch spectral state. The two power spectra are quite similar. Note the steepness of the very low frequency component in the power spectrum of the Rapid Burster, which is due to the presence of type II bursts.

c) Some Speculation on Type II Burst Models

The observation of an “odd-even effect” in the presence of ~ 5 Hz QPOs during consecutive peaks of the time-invariant structure in the bursts of ~ 10 s duration (see § IIIc) may imply a link between these two phenomena (as argued in § IIIc, it is unlikely that the time scale-invariant profile is simply a very low frequency extension of the QPO). Based on this observation, we will in the following paragraphs outline a scenario that may connect some hitherto unrelated phenomena observed in the Rapid Burster. Our considerations are very qualitative and speculative.

Our point of departure is the basic “relaxation oscillator” model, which is forced upon us by the observed relation between burst fluence and waiting time until the next burst (Lewin *et al.* 1976). According to this generally accepted model for the type II bursts, the Rapid Burster contains a “reservoir” in which inflowing matter (from the accretion disk) accumulates, until a “critical level” in some physical parameter is reached. When this happens, a leak suddenly develops in the reservoir, and matter can accrete onto the neutron star. As a result of this sudden accretion (which gives rise to a type II burst), the reservoir loses matter by an amount that is proportional to the fluence in the burst. At a constant rate of refilling of the reservoir by new matter following in from outside, the time interval it takes to reach the critical trigger level again, i.e., the time interval to the next burst, is therefore proportional to the size of the previous burst. It is possible that the reservoir of matter is supported, and prevented from accreting directly, by the magnetic field of the neutron star; magnetospheric models for the Rapid Burster have been discussed in some detail by, e.g., Baan (1977, 1979), Michel (1977), Lamb *et al.* (1977), Davidson (1982), and by Hanawa, Hirotani, and Kawai (1989).

We envisage that this reservoir has a “bottom,” whose height above the neutron star can vary on time scales of seconds and longer. The introduction of this property was stimulated by our attempts to account for another striking, but so far unexplained, feature of the Rapid Burster, i.e., the dips in the persistent emission which are often seen just before and after a type II burst (van Paradijs, Cominsky, and Lewin 1979; Stella *et al.* 1988b). These dips show that one way or another the system knows a burst is about to come (i.e., the reservoir is nearly filled), and informs us of this by a temporary suppression of the persistent emission.

We speculate that at least part of the persistent emission is caused by “spillover” from the top of the reservoir; this matter reaches the neutron star along a route which differs from that taken by matter that accretes (though the bottom of the reservoir) during the bursts. Within the framework of low-mass X-ray binaries as harboring weakly magnetized neutron stars, it is natural to think of this alternative accretion route as a flow toward the magnetic poles (the top of the reservoir being located near, but outside, the magnetopause around the neutron star), as compared to inflow, e.g., in the equatorial plane of the neutron star. Continuing our speculation, we assume that when the reservoir is nearly filled, its bottom starts to sink, so that it becomes more difficult for matter from the top part of the reservoir (spillover) to reach the neutron star via the polar route; the persistent flux decreases.

We note that this scenario for the preburst dips encounters a potential problem that exists for all models of low-mass X-ray binaries involving magnetospheres: no pulsations have ever

been detected (see Lewin, van Paradijs, and van der Klis 1988 for a recent summary). Various possible mechanisms have recently been proposed to suppress X-ray pulsations in luminous low-mass X-ray binaries (Bussard *et al.* 1988; Brainerd and Lamb 1987; Kylafis and Klimis 1987; Wang and Schlickeiser 1987; Meszaros, Riffert, and Berthiaume 1988; Wood, Ftacilas, and Kearney 1988).

Radial motion (up and down) of the bottom of the reservoir during the burst leaves room for the possibility of intervals of increased leakage with less spillover (the bottom of the reservoir is then located relatively deeply, possibly within the magnetopause; accretion occurs preferentially near the equatorial regions of the neutron star), alternating with intervals of less leakage but increased spillover from the top of the reservoir. Since during the consecutive peaks in the type II bursts the accretion geometry changes from dominance of accretion via the polar regions of the magnetosphere to dominance of accretion near the equatorial plane, this scenario of an

oscillating bottom of the reservoir allows, in principle, for the possibility of an odd-even effect in the QPO properties during consecutive peaks in the time-invariant burst profile.

We note, finally, that although our above speculation on the properties of the reservoir may eventually lead to an expansion of the “odd-even” behavior of the QPO, it contributes little to answering the important question as to what it is that makes this source so unique.

J. v P. and W. P. acknowledge support from the Netherlands Ministry of Education and Research, the Netherlands Foundation for the Advancement of Research (NWO), and the Leids Kerkhoven-Boscha Fonds. They thank the Institute for Space and Astronautical Science for the hospitality during their stay there, when part of the work presented here was performed. W. H. G. L. is supported by the National Aeronautics and Space Administration, under contracts NAG8-571, NAG8-674, and NSG-7643.

REFERENCES

- Alpar, M. A., and Shaham, J. 1985, *Nature*, **316**, 239.
 Baan, W. 1977, *Ap. J.*, **214**, 245.
 ———, 1979, *Ap. J.*, **227**, 987.
 Basinska, E. M., Lewin, W. H. G., Cominsky, L., van Paradijs, J., and Marshall, F. 1980, *Ap. J.*, **241**, 787.
 Brainerd, J., and Lamb, F. K. 1987, *Ap. J. (Letters)*, **317**, L33.
 Bussard, R. W., Weisskopf, M. C., Elsner, R. F., and Shinazaki, N. 1988, *Ap. J.*, **327**, 284.
 Davidson, G. T. 1982, *Ap. J.*, **255**, 705.
 Dotani, T. 1989, Ph.D. thesis, University of Tokyo.
 Hanawa, T., Hirofani, K., and Kawai, N. 1989, *Ap. J.*, **336**, 920.
 Hasinger, G. 1986, in *IAU Symposium 125, The Origin and Evolution of Neutron Stars*, ed. D. J. Helfand and J. H. Huang (Dordrecht: Reidel), p. 333.
 ———, 1987, *Astr. Ap.*, **186**, 153.
 Hasinger, G., and van der Klis, M. 1989, *Astr. Ap.*, in press.
 Hoffman, J. A., Marshall, H., and Lewin, W. H. G. 1978, *Nature*, **271**, 630.
 Inoue, H., *et al.* 1980, *Nature*, **283**, 358.
 Kawai, N. 1985, Ph.D. thesis, University of Tokyo.
 Kawai, N., Matsuoka, M., Inoue, H., Ogawara, Y., Tanaka, Y., Kunieda, H., and Tawara, Y. 1988, *Pub. Astr. Soc. Japan*, submitted.
 Kunieda, H., *et al.* 1984a, *Pub. Astr. Soc. Japan*, **36**, 215.
 ———, 1984b, *Pub. Astr. Soc. Japan*, **36**, 807.
 Kylafis, N. D., and Klimis, G. S. 1987, *Ap. J.*, **323**, 678.
 Lamb, F. K. 1990, *Ap. J.*, submitted.
 Lamb, F. K., Fabian, A. C., Pringle, J. E., and Lamb, D. Q. 1977, *Ap. J.*, **217**, 197.
 Lamb, F. K., Shibasaki, N., Alpar, M. A., and Shaham, J. 1985, *Nature*, **317**, 681.
 Lewin, W. H. G., *et al.* 1976, *Ap. J. (Letters)*, **207**, L95.
 Lewin, W. H. G., van Paradijs, J., and van der Klis, M. 1988, *Space Sci. Rev.*, **47**, 273.
 Makino, F., *et al.* 1987, *Ap. Letters Comm.*, **25**, 233.
 Marshall, H. L., Ulmer, M. P., Hoffman, J. A., Doty, J., and Lewin, W. H. G. 1979, *Ap. J.*, **227**, 555.
 Meszaros, P., Riffert, H., and Berthiaume, G. 1988, *Ap. J.*, **325**, 204.
 Michel, F. C. 1977, *Ap. J.*, **216**, 838.
 Middleditch, J., and Priedhorsky, W. C. 1986, *Ap. J.*, **306**, 230.
 Mitsuda, K. 1988a, in *Physics of Neutron Stars and Black Holes*, ed. Y. Tanaka (Tokyo: Universal Academic Press), p. 117.
 ———, 1988b, talk presented at the Fifth Los Alamos Space Physics/Astrophysics Workshop on Quasi-periodic Oscillations in Luminous Galactic X-Ray Sources, La Cienaga, New Mexico, 1988 October.
 Mitsuda, K., and Dotani, T. 1989, *Pub. Astr. Soc. Japan*, **41**, 557.
 Mitsuda, K., Inoue, H., Nakamura, N., and Tanaka, Y. 1989, *Pub. Astr. Soc. Japan*, **41**, 97.
 Nishimura, J., Mitsuda, K., and Itoh, M. 1986, *Pub. Astr. Soc. Japan*, **38**, 819.
 Stella, L. 1988, talk presented at the Fifth Los Alamos Space Physics/Astrophysics Workshop on Quasi-periodic Oscillations in Luminous Galactic X-Ray Sources, La Cienaga, New Mexico, 1988 October.
 Stella, L., Haberl, F., Lewin, W. H. G., Parmar, A. N., van der Klis, M., and van Paradijs, J. 1988a, *Ap. J. (Letters)*, **327**, L13.
 Stella, L., Haberl, F., Lewin, W. H. G., Parmar, A. N., van Paradijs, J., and White, N. E. 1988b, *Ap. J.*, **324**, 379.
 Tan, J., *et al.* 1989, in preparation.
 Tawara, Y., Hayakawa, S., Kunieda, H., Makino, F., and Nagase, F. 1982, *Nature*, **299**, 38.
 Tawara, Y., Kawai, N., Tanaka, Y., Inoue, H., Kunieda, H., and Ogawara, Y. 1985, *Nature*, **318**, 545.
 Turner, M. J. L., *et al.* 1989, *Pub. Astr. Soc. Japan*, **41**, 345.
 van der Klis, M. 1986, in *Lecture Notes in Physics*, Vol. **266**, *The Physics of Accretion onto Compact Objects*, ed. M. G. Watson, K. O. Mason, and N. White (Berlin: Springer), p. 157.
 ———, 1989, *Ann. Rev. Astr. Ap.*, **27**, 517.
 van der Klis, M., Jansen, F., van Paradijs, J., Lewin, W. H. G., van den Heuvel, E. P. J., Truemper, J., and Sztajno, M. 1985, *Nature*, **316**, 225.
 van Paradijs, J., Cominsky, L., and Lewin, W. H. G. 1979, *M.N.R.A.S.*, **189**, 387.
 Wang, Y.-M., and Schlickeiser, R. 1987, *Ap. J.*, **313**, 200.
 Wood, K. S., Ftacilas, C., and Kearney, M. 1988, *Ap. J.*, **324**, 466.

T. DOTANI, H. INOUE, K. MITSUDA, and Y. TANAKA: Institute of Space and Astronautical Science, 1-1 Yoshinodai 3-chome, Sagamihara, Kanagawa 229, Japan

N. KAWAI: Cosmic Radiation Laboratory, RIKEN Institute of Physical and Chemical Research, 2-1 Hirosawa, Wako, Saitama 351-01, Japan

K. MAKISHIMA: Department of Physics, University of Tokyo, 7-3-1 Hongo, Bunkyo-ky, Tokyo 113, Japan

W. PENNINX, M. VAN DER KLIS, and J. VAN PARADIJS: Astronomical Institute “Anton Pannekoek,” University of Amsterdam, Roetersstraat 15, 1018 WB Amsterdam, the Netherlands

J. TAN and W. H. G. LEWIN: Center for Space Research and Department of Physics, Massachusetts Institute of Technology 37-627, Cambridge, MA 02137

Y. TAWARA: Department of Astrophysics, Faculty of Science, Nagoya University, Furo-chu, Chikusa-ku, Nagoya 464, Japan